[16] G. Eglinton, A. R. Galbraith, *J. Chem. Soc.* **1959**, 889 – 896.
[17] a) A. S. Hay, *J. Org. Chem.* **1962**, *27*, 3320 – 3321; b) K. Okuhara, *Bull. Chem. Soc. Jpn.* **1981**, *54*, 2045 – 2052.
[18] C. Heim, Diploma thesis, University of Würzburg, **1995**. Typically, ^{1}H NMR spectra showed small signals at $\delta = 3.0 - 3.5$, and the IR spectra weak absorptions at $\tilde{\nu} = 3300 - 3350\ cm^{-1}$ which indicate the presence of terminal acetylenic units. MALDI-TOF mass spectra revealed various peak pairs with a mass difference of m/z 2 corresponding to linear and cyclic oligomers of the same number of repeating units.
[19] D. O'Krongly, S. R. Denmade, M. Y. Chiang, R. Breslow, *J. Am. Chem. Soc.* **1985**, *107*, 5544 – 5545.
[20] Representative physical data of the oligothiophenediyne macrocycles: **13**: ^{1}H NMR ($CDCl_3$): $\delta = 7.07$ (s, 6H, thiophene (Th)-H), 2.66 (m, 24H, α-CH_2), 1.49 (m, 48H, β,γ-CH_2), 0.97 (m, 36H, CH_3); ^{13}C NMR ($CDCl_3$): $\delta = 149.63$, 138.32, 136.71, 133.73, 124.87 (α,β-Th-C), 117.12 (α-Th-C), 81.92 (C≡C), 78.63 (C≡C), 32.66, 32.38 (β-CH_2), 28.74, 27.64 (α-CH_2), 22.96, 22.69 (γ-CH_2), 13.88 (CH_3); m.p. $> 300\,^\circ$C; MALDI-TOF-MS: m/z: 1554.8 [M^+]. **15**: ^{1}H NMR ($CDCl_3$): $\delta = 7.10$ (d, 6H, Th-H), 7.09 (d, 6H, Th-H), 2.71 (m, 36H, α-CH_2), 1.54 (m, 72H, β,γ-CH_2), 0.99 (m, 54H, CH_3); ^{13}C NMR ($CDCl_3$): $\delta = 150.99$, 140.35, 138.50, 136.84, 135.71, 133.59, 129.96, 126.24, 125.71 (α,β-Th-C), 116.62 (α-Th-C), 81.44, 78.01 (C≡C), 32.82, 32.63, 31.58 (β-CH_2), 28.69, 27.90, 27.69 (α-CH_2), 23.03, 22.94, 22.71 (γ-CH_2), 13.87 (CH_3); m.p. 203 – 204 °C; MALDI-TOF-MS: m/z: 2386 [M^+].
[21] J. J. P. Stewart, MOPAC Program Package, QCPE 455, Indiana University.
[22] a) A. Carpita, R. Rossi, C. A. Veracini, *Tetrahedron* **1985**, *41*, 1919 – 1929; b) D. M. Perrnie, J. Kagan, *Heterocycles* **1986**, *24*, 365 – 368.
[23] Representative physical data of the cyclo[n]thiophenes **17** – **19**: **17**: ^{1}H NMR ($CDCl_3$): $\delta = 7.06$ (s, 12H, Th-H), 2.70 (t, 24H, α-CH_2), 1.42 (m, 48H , β,γ-CH_2), 0.95 (t, 36H, CH_3); ^{13}C NMR ($CDCl_3$): $\delta = 140.31$ (β-Th-C), 136.55, 130.07 (α-Th-C), 125.43 (β-Th-C), 32.80 (β-CH_2), 27.80 (α-CH_2), 23.01 (γ-CH_2), 13.88 (CH_3); m.p. $> 250\,^\circ$C; MALDI-TOF-MS: m/z: 1656.80 [M^+]. **18**: ^{1}H NMR ($CDCl_3$): $\delta = 7.09$ (s, 16H, Th-H), 2.69 (t, 32H, α-CH_2), 1.45 (m, 64H , β,γ-CH_2), 0.97 (t, 48H, CH_3); m.p. $> 250\,^\circ$C; MALDI-TOF-MS: m/z: 2210.81 [M^+]. **19**: ^{1}H NMR ($CDCl_3$): $\delta = 7.10$ (s, 18H, Th-H), 2.75 (t, 36H, α-CH_2), 1.54 (m, 36H, β-CH_2), 1.47 (m, 36H, γ-CH_2), 0.99 (t, 54H, CH_3); ^{13}C NMR ($CDCl_3$): $\delta = 140.11$ (β-Th-C), 136.18, 129.98 (α-Th-C), 125.72 (β-Th-C), 32.86 (β-CH_2), 27.94 (α-CH_2), 23.06 (γ-CH_2), 13.90 (CH_3); m.p. 210 °C; MALDI-TOF-MS: m/z: 2486 [M^+].
[24] H. Plenio, *Angew. Chem.* **1997**, *109*, 358 – 360; *Angew. Chem. Int. Ed. Engl.* **1997**, *36*, 348 – 350.
[25] Crystal data: $C_{128}H_{82}S_{12}$, $M_r = 2004.66$, triclinic, space group $P\bar{1}$, $a = 11.914(3)$, $b = 16.444(3)$, $c = 17.749(4)$ Å, $\alpha = 113.17(2)$, $\beta = 98.40(3)$, $\gamma = 104.63(3)^\circ$, $V = 2973.0$ Å^3, $Z = 1$, $\rho_{calcd} = 1.120\ g\,cm^{-3}$, crystal dimensions $0.11 \times 0.22 \times 0.53$ mm, $T = 293(2)$ K, $\mu = 0.266\ mm^{-1}$. Intensity data were collected on a STOE-IPDS image-plate diffractometer ($Mo_{K\alpha}$ radiation ($\lambda = 0.71073$ Å), graphite monochromator) in the φ rotation scan mode, $\theta_{max} = 26^\circ$, 23195 reflections measured, 10776 unique reflections were measured and used in the refinement. Lorentz and polarization correction. The structure was solved by direct methods (XMY93 program system: T. Debaerdemaeker, *Z. Kristallogr.* **1993**, *206*, 173 – 182). The molecule is located on a crystallographic inversion centre. Refinement (SHELXL97; G. M. Sheldrick, University of Göttingen, **1993**) of positional and anisotropic thermal parameters for all non-hydrogen atoms converged to $R1 = 0.1446$ ($wR2 = 0.3344$) for 1483 reflections with $I \geq 2\sigma(I)$. No attempt was made to locate the hydrogen atoms. The relatively poor R value is probably a result of the large disorder in some of the butyl chains. Unfortunately, no suitable crystals were available for data collection at low-temperature. Crystallographic data (excluding structure factors) for the structures reported in this paper have been deposited with the Cambridge Crystallographic Data Centre as supplementary publication no. CCDC-142083. Copies of the data can be obtained free of charge on application to CCDC, 12 Union Road, Cambridge CB2 1EZ, UK (fax: (+44) 1223-336-033; e-mail: deposit@ccdc.cam.ac.uk).
[26] F. Diederich, Y. Rubin, *Angew. Chem.* **1992**, *104*, 1123 – 1146; *Angew. Chem. Int. Ed. Engl.* **1992**, *31*, 1101 – 1123.
[27] H. Ueda, C. Katayama, J. Tanaka, *Bull. Chem. Soc. Jpn.* **1981**, *54*, 891 – 896.
[28] A. Bondi, *J. Phys. Chem.* **1964**, *68*, 441.
[29] a) R. Azumi, G. Götz, T. Debaerdemaeker, P. Bäuerle, *Chem. Eur. J.* **2000**, *6*, 735 – 744; b) T. Kirschbaum, R. Azumi, E. Mena-Osteritz, P. Bäuerle, *New J. Chem.* **1999**, *23*, 241 – 251; c) M. S. Vollmer, F. Effenberger, R. Stecher, B. Gompf, W. Eisenmenger, *Chem. Eur. J.* **1999**, *5*, 96 – 101; d) H. Müller, J. Petersen, R. Strohmaier, B. Gompf, W. Eisenmenger, M. S. Vollmer, F. Effenberger, *Adv. Mater.* **1996**, *8*, 733 – 737; e) P. Bäuerle, T. Fischer, B. Bidlingmeier, A. Stabel, J. P. Rabe, *Angew. Chem.* **1995**, *34*, 335 – 339; *Angew. Chem. Int. Ed. Engl.* **1995**, *34*, 303 – 307; f) A. Stabel, J. P. Rabe, *Synth. Met.* **1994**, *67*, 47 – 53.
[30] The STM images were recorded at ambient temperature with the aid of low-current STM (RHK) regulated by a RHK STM-1000 control system equipped with a mechanically cut Pt/Ir tip. All of the images presented were obtained at quasi-constant height in the variable current mode without further manipulation or using a voltage pulse in order to induce the ordering, and without digital image processing. The bias voltages were typically around -400 to -450 mV and the setpoint currents around 0.3 – 0.5 nA. A freshly cleaved surface of HOPG was first carefully characterized under ambient conditions, then solutions of the macrocycles in 1,2,4-trichlorobenzene were deposited onto the substrate. In situ STM imaging of the self-assembled 2D monolayers was performed at the interface between HOPG and concentrated solutions of the macrocycles.

Investigating the Surface Morphology of Triacontyl Phases with Spin-Diffusion Solid-State NMR Spectroscopy**

Martin Raitza, Jürgen Wegmann, Stefan Bachmann, and Klaus Albert*

The detailed characterization of molecular recognition structures is one of the essential prerequisites for the development of new materials for specific applications in catalysis, sensor technology, and for the analysis of mixtures of compounds.

Highly selective stationary phases are needed for the efficient separation of complex mixtures of compounds in high-performance liquid chromatography (HPLC).[1] The tailored synthesis of these phases is impossible without any detailed knowledge of the surface structure of the materials and a detailed understanding of the structural and dynamic properties of the separation phase. Routine applications in HPLC can be successfully performed with reversed-phase materials,[2] which are prepared by modifying silica gel with *n*-alkylsilanes (for example, *n*-octadecylsilane). Reversed phas-

[*] Prof. Dr. K. Albert, Dr. M. Raitza, Dipl.-Chem. J. Wegmann, Dipl.-Chem. S. Bachmann
Institut für Organische Chemie der Universität Tübingen
Auf der Morgenstelle 18, 72076 Tübingen (Germany)
Fax: (+49) 7071-295875
E-mail: klaus.albert@uni-tuebingen.de

[**] This work was funded by the Deutsche Forschungsgemeinschaft (FOR 184/3-1) and the Fonds der Chemischen Industrie. We thank Bischoff Analysentechnik und -geräte GmbH, Leonberg, Germany for providing ProntoSIL silica gel.

  1433-7851/00/3919-3486 $ 17.50+.50/0

es with triacontyl chains show an extremely high shape selectivity for the separation of stereoisomers (for example, β-carotene stereoisomers).[3–5] Solid-state NMR spectroscopy is of great importance for the characterization of these amorphous compounds and through the many experiments possible delivers valuable information on the structural and dynamic behavior.

Reversed phases with high shape selectivity can be prepared by the solution polymerization procedure, in which a defined quantity of water is added during the modification reaction of silica gel with *n*-alkylsilanes. Solid-state ^{13}C NMR investigations of these materials reveal two signals for the methylene groups of the alkyl chain which can be assigned to one domain with preferentially all *trans* and the other one with mainly *gauche* conformations. Many investigations performed with "self-assembled monolayers" (SAMs) reveal that the observed signal splitting also takes place in diverse *n*-alkyl-modified inorganic oxides (Al_2O_3, SiO_2, TiO_2, and ZrO_2).[6–9] No information could be gained up to now upon the size, extension, and alignment of these domains, even though these parameters are responsible for the selectivity of the chromatographic separation.[4, 10–16] The main question which still remains is what is the alignment of the domains: there could be a lateral alignment with the island structures at the silica surface or a mobility gradient along the alkyl chains with layers parallel to the silica surface.

The answer to this question can be found by employing spin-diffusion solid-state NMR investigations. These experiments have large practical applications for the determination of the homogeneity of polymers and have been mainly conducted to determine the phase structure of organic polymers.[17–19] Moreover, the alignment and size of domains of different mobility can be determined in the range of 5 to 2000 Å. The basic principle of the method is outlined in Figure 1.[18] The magnetization of the sample is shown in the

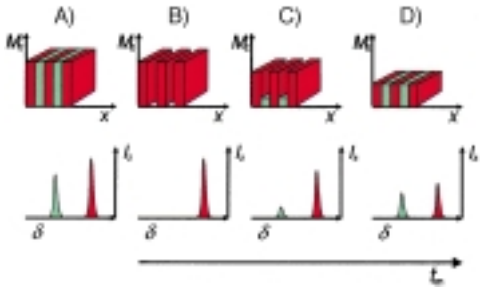

Figure 1. Schematic representation of the principle of spin-diffusion experiments. Top: sample magnetization, bottom: NMR spectra; red: mobile, green: rigid; A – B: selection, B – D: spin diffusion, t_m: mixing time.

upper part of Figure 1, while the lower part depicts the resulting NMR spectra. The sample under investigation consists of two domains with different mobility, which are indicated by different colors (red: mobile, green: rigid).

At the start of the NMR experiment the sample is in state A where the magnetization is distributed in both domains, and results in NMR signals of both domains. In a second step a selection process is performed by making use of the different relaxation times.[20, 21] Thus in state B only one component of the sample contains a significant magnetization, which is registered in the NMR spectrum. Spin diffusion starts at state B, that is, magnetization is transferred to neighboring nuclei by dipolar interactions and thus starts to diffuse. During this diffusion mixing time t_m the magnetization of mobile compounds decreases while the magnetization of rigid nonselected components increases again. Thus, the intensity of the signal corresponding to the mobile species in the NMR spectrum decreases while the second signal increases in intensity (state C). Finally the magnetization in the equilibrium state D is distributed on both components and the NMR spectra are similar to those of state A but show less signal intensity.

The reduction in the magnetization during the spin-diffusion mixing time t_m can be used to understand the distribution, that is, the size of areas of equal mobility. If the distribution of both components at the silica surface is very homogeneous, then a large number of border areas exist between domains with different mobility. Interactions between both components take place at these border areas and the equilibrium state can be reached very fast. A more uneven distribution with big domains of equal mobility results in less border areas and the adjustment of the magnetization takes more time.

Figure 2 shows the pulse sequence of the spin-diffusion experiment together with the application of the dipolar filter. First a 12 pulse block consisting of 90° pulses in the proton

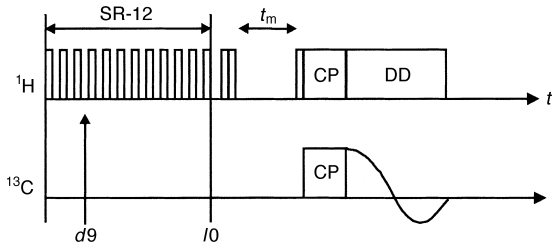

Figure 2. Schematic representation of the pulse sequence for the spin-diffusion experiment with a dipolar filter and ^{13}C detection. *l*0: number of repetitions of the 12 pulse sequence, *d*9: delay time between two 90° pulses, t_m: variable mixing time.

channel is applied, which eliminates the dipolar couplings of the protons in the mobile component. Thus, there is only a very small dephasing of the magnetization of the mobile components, while a fast dephasing of the magnetization of the rigid components takes place because of the strong dipole interactions. The delay times *d*9 between the single pulses and the number of repetitions of the pulse block *l*0 are parameters which can be varied for an optimal selection according to the nature of the investigated sample. Two 90° pulses follow, which alternately align the magnetization to the $+z$ or $-z$ axis of the corresponding phase cycles, in order to correct for T_1 effects. Spin diffusion takes place following the mixing time t_m, and is followed by the cross-polarization pulse sequence, and detection in the ^{13}C channel. Rows of spectra are registered by incrementing the mixing time t_m, which enables the time dependence of the diffusion to be studied by observing changes in the signal intensity.

  1433-7851/00/3919-3487 $ 17.50+.50/0

Figure 3 shows the ^{13}C CP/MAS NMR spectra of a triacontyl separation phase recorded with mixing times t_m of the spin-diffusions experiment varied between 1 μs and

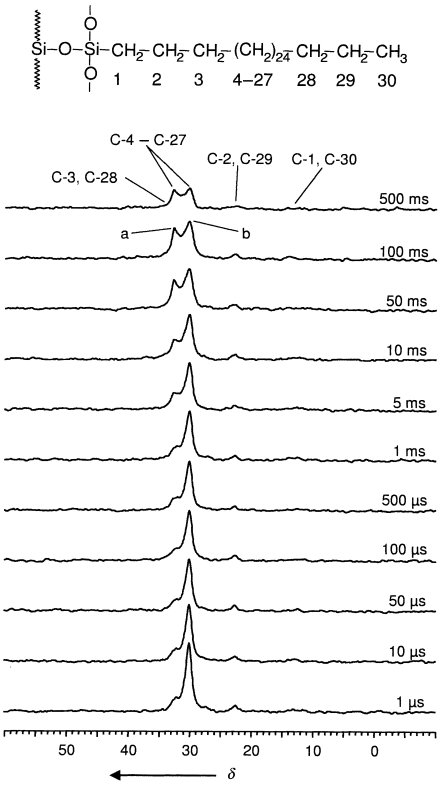

Figure 3. Spin-diffusion NMR experiment with ^{13}C detection of a C_{30} phase (ProntoSIL 3 μm, 200 Å, surface coverage 3.5 μmol m^{-2}) with a varible mixing time t_m and a temperature of 312 K ($l0 = 6$, $d9 = 10$ μs); a: rigid, b: mobile.

500 ms. Two resonances at $\delta = 32.8$ and 30.0 are observed for the carbon atoms of the methylene chain. These signals can be assigned to rigid all-*trans* and mobile *gauche* conformations, respectively, of the alkyl chain.[14] The spectrum with the smallest mixing time t_m of 1 μs clearly depicts that only mobile domains exhibit a reasonable magnetization at the start of the spin-diffusion experiment, since only the high-field-shifted signal $\delta = 30.0$ is visible. Spin diffusion becomes more effective with increasing mixing time, and magnetization is transferred from the mobile to rigid domains. Thus the signal at $\delta = 30.0$ decreases in intensity whereas the signal at $\delta = 32.8$ increases in intensity. At the largest employed mixing time t_m of 500 ms both signals show comparable intensity. The decrease in the intensity of the signals of the carbon atoms of the mobile alkyl chains together with the increase in intensity of signals for the carbon atoms of the rigid alkyl chains corresponds to the tranfer of magnetization from the mobile to the rigid alkyl-chain domains.

This phenomenon is direct proof for the existence of alkyl-chain domains of different mobility at the silica surface of C_{30} reversed phases, which are prepared under the special solution polymerization procedure. The distribution of the domains can be derived from the time dependence of the signal decay of the methylene chains recorded during the spin-diffusion experiment. Domains parallel to the silica surface, which result from a mobility gradient from the silica surface to the end of the alkyl chain, should exhibit a very fast spin diffusion. This effect is in accordance with the hypothesis of a lateral distribution of domains, that is, island structures are formed at the silica surface. These different regions are caused by the different cross-linking of the silanes employed during the synthetic procedure. Thus clusters are formed from an array of closely packed C_{30} alkyl chains which bind to the silica surface and are organized in rigid domains.

The size of the domains can be estimated by comparing the decrease of the signal at $\delta = 30.0$ with the signal progression derived from a simulated spin-diffusion experiment. Here the whole sample is represented by a periodic array of quadratic single cells which exhibit different mobility and are mixed together (core/shell model; Figure 4, top). The system is

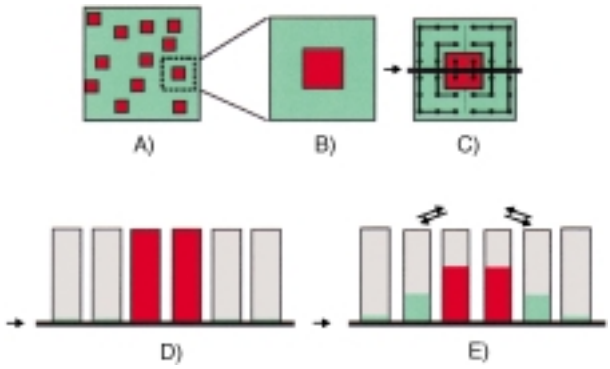

Figure 4. Schematic representation of the sample model (A). It was hypothesized that the sample consists of a periodic array of unit cells (B). The two-dimensional spin lattice (C) is projected into one dimension (D, E).

projected with respect to symmetry considerations into one dimension by summation of the lattice points that are able to receive magnetization. Thus the one-dimensional display contains marked lattice points at regular distances which are able to take up magnetization and to exchange with their neighbors (Figure 4, bottom). The whole system reaches the equilibrium state as a result of the different sizes of the two domains.

The size of the diffusion constant is important for the simulation of the spin-diffusion process. In earlier publications this process has been independently addressed and a diffusion constant in the range of 20–100 Å^{2}ms^{-1} was determined.[17, 21–24] A diffusion constant $D_m = 30$ Å^{2}ms^{-1} for the mobile component and of $D_r = 80$ Å^{2}ms^{-1} for the rigid component was used for the interpretation of the current system. Figure 5 shows the comparison of the experimental data together with the simulated reduction. The signals (Figure 3) were simulated by peak deconvolution by employing Lorentian peak shapes. The intensity of the signal of the mobile component is related to the integral value of both signals, which corresponds to 100. A good fit with the experimental data is obtained with values of 112 Å for the core of the single cell (mobile component $D_m = 30$ Å^{2}ms^{-1}) and 16 Å for the shell of the unit cell (rigid component, $D_m =$ 80 Å^{2}ms^{-1}). A calculation of the relative areas of both

  1433-7851/00/3919-3488 $ 17.50+.50/0

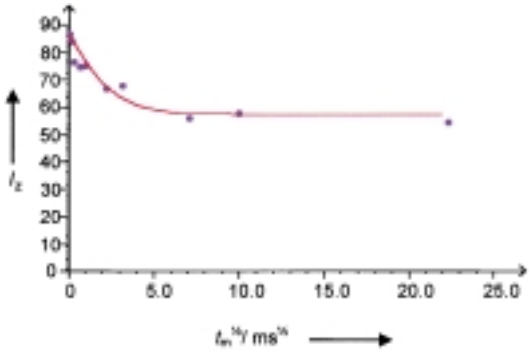

Figure 5. Comparison of the experimental decrease in the signal of the mobile component and the simulated curve with respect to the mixing time (ProntoSIL 3 μm, 200 Å, surface coverage 3.5 μmol m^{-2}).

components for one unit cell is possible from the proposed structure and arrangement of unit cells (Figure 4). An area of (112 Å)^2 ≈ 12 500 Å^2 (red area) results for the mobile component and an area of (16 Å + 112 Å + 16 Å)^2 − (112 Å)^2 ≈ 8200 Å^2 (green area) for the rigid component. Thus the ratio of the mobile:rigid area is 60:40.

Thus it is clear that two domains exist with different densities of alkyl chains and their sizes can be evaluated. The model depicted in Figure 6 results from the described

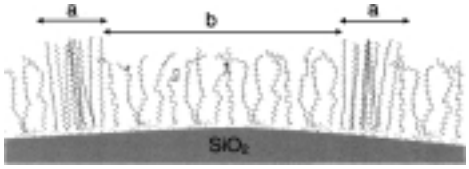

Figure 6. Model of the silica surface of a C_{30} phase chemically modified with trichlorotriacontylsilane. Region a: rigid, 32 Å; region b: mobile, 112 Å.

measurements together with the computer simulation. Thus an average domain size of 8200 Å^2 for the rigid all-*trans* alkyl-chain conformations (average alkyl-chain length 43 Å) and of 12 500 Å^2 for the *gauche* alkyl-chain domains (average alkyl-chain length 31 Å) can be concluded. Thus it was possible to derive insight into the spatial distribution of alkyl chains at the silica surface by employing the outlined solid-state NMR experiments. Direct proof of the existence of C_{30} alkyl chain domains with different mobility at the silica surface was obtained in the case of the investigated C_{30} reversed-phase spin-diffusion measurements.

Experimental Section

The investigated C_{30} phase was synthesized according to the solution polymerization procedure[14]. Silica gel (ProntoSIL, particle size 3 μm, pore size 200 Å, Bischoff Analysentechnik und -geräte GmbH, Leonberg, Germany) was dried under vacuum conditions at 180° for 4 h, suspended in xylene, and treated with a threefold excess of triacontyltrichlorosilane. The polymerization was started by the addition of a defined amount of water and the reaction mixture was heated at reflux overnight. A white powder was obtained after purification of the product.

NMR parameters: The NMR spectra were recorded on a Bruker ASX 300 spectrometer. ^{13}C CP/MAS NMR measurements were performed with a 7-mm probe at a spinning rate of 4000 Hz and a sample temperature of 312 K (90° pulse angle 6.5 μs, 2048 transients, contact time 6 ms, delay time 1 s, time domain 2 K data points with a spectral width (SW) of 23 kHz, acquisition time 45 ms).

Spin-diffusion MAS NMR measurements were recorded with the dipolar filter with six repetition cycles (*l*0) and a delay time of 10 μs (*d*9) between the ^{1}H pulses. A 7-mm probe was employed at a spinning rate of 4000 Hz and a sample temperature of 312 K (90° pulse angle 6.9 μs, 12 288 transients, contact time 6 ms, delay time 1 s, time domain 2 K data points with a spectral width (SW) of 23 kHz, acquisition time 45 ms).

The simulation of the spin diffusion was performed with a self-developed computer programm (MR-SpinDiff) on a PC (Pentium, 200 MHz).

Received: April 4, 2000 [Z 14941]

[1] K. K. Unger in *Packings and Stationary Phases in Chromatographic Techniques*, *Vol. 47* (Ed.: K. K. Unger), Marcel Dekker, New York, **1990**.
[2] W. R. Melander, C. Horvath, *High Performance Liquid Chromatography*, *Vol. 2*, Academic Press, New York, **1980**, p. 113.
[3] L. C. Sander, K. Epler Sharpless, N. E. Craft, S. A. Wise, *Anal. Chem.* **1994**, *66*, 1667 – 1674.
[4] M. Pursch, S. Strohschein, H. Händel, K. Albert, *Anal. Chem.* **1996**, *68*, 386 – 393.
[5] S. Strohschein, M. Pursch, H. Händel, K. Albert, *Fresenius J. Anal. Chem.* **1997**, *357*, 498 – 502.
[6] W. Gao, L. Reven, *Langmuir* **1995**, *11*, 1860 – 1863.
[7] W. Gao, L. Dickinson, C. Grozinger, F. G. Morin, L. Reven, *Langmuir* **1996**, *12*, 6429 – 6435.
[8] W. Gao, L. Dickinson, C. Grozinger, F. G. Morin, L. Reven, *Langmuir* **1997**, *13*, 115 – 118.
[9] M. Pursch, L. C. Sander, K. Albert, *Anal. Chem.* **1996**, *68*, 4107 – 4113.
[10] K. Albert, B. Evers, E. Bayer, *J. Magn. Reson.* **1985**, *62*, 428 – 436.
[11] M. Pursch, R. Brindle, A. Ellwanger, L. C. Sander, C. M. Bell, H. Händel, K. Albert, *Solid-State NMR* **1997**, *9*, 191 – 201
[12] M. Pursch, L. C. Sander, H.-J. Egelhaaf, M. Raitza, S. A. Wise, D. Oelkrug, K. Albert, *J. Am. Chem. Soc.* **1999**, *121*, 3201 – 3213.
[13] K. Albert, A. Ellwanger, M. Dachtler, T. Lacker, S. Strohschein, J. Wegmann, M. Pursch, M. Raitza in *Fundamentals and Applied Aspects of Chemically Modified Surfaces*, *Vol. 7* (Eds.: J. Blitz, C. Little), The Royal Society of Chemistry, Cambridge, **1999**, pp. 111 – 128.
[14] K. Albert, T. Lacker, M. Raitza, M. Pursch, H.-J. Egelhaaf, D. Oelkrug, *Angew. Chem.* **1998**, *110*, 809 – 812; *Angew. Chem. Int. Ed.* **1998**, *37*, 777 – 780.
[15] K. Albert, *Trends Anal. Chem.* **1998**, *17*, 648 – 658.
[16] M. Raitza, M. Pursch, S. Strohschein, L. C. Sander, K. Albert, *GIT Lab. J.* **1998**, *4*, 237 – 241.
[17] J. Clauss, K. Schmidt-Rohr, A. Adam, C. Boeffel, H. W. Spiess, *Macromolecules* **1992**, *25*, 5208 – 5214.
[18] K. Schmidt-Rohr, H. W. Spiess, *Multidimensional Solid State NMR and Polymers*, Academic Press, San Diego, **1994**, pp. 402 – 439.
[19] F. Mellinger, M. Wilhelm, K. Landfester, H. W. Spiess, A. Haunschild, J. Packusch, *Acta Polym.* **1998**, *49*, 108 – 115.
[20] M. Goldman, L. Shen, *Phys. Rev.* **1961**, *144*, 321 – 328.
[21] J. Clauss, K. Schmidt-Rohr, H. W. Spiess, *Acta Polym.* **1993**, *44*, 1 – 17.
[22] T. Kimura, K. Neki, N. Tamura, F. Horii, M. Nakagawa, H. Odani, *Polymer* **1992**, *33*, 493 – 497.
[23] M. Ishida, K. Yoshinaga, F. Horii, *Macromolecules* **1996**, *29*, 8824 – 8829.
[24] R. R. Eckman, P. M. Henrichs, A. J. Peacock, *Macromolecules* **1997**, *30*, 2474 – 2481.

  1433-7851/00/3919-3489 $ 17.50+.50/0